

**HETEROGENEOUS CATALYSTS FROM RICE  
HUSK MODIFIED WITH CHROMIUM,  
MOLYBDENUM AND TUNGSTEN: SYNTHESIS,  
CHARACTERIZATION AND APPLICATION IN  
STYRENE OXIDATION**

MOHAMMAD ANWAR BIN MOHAMED IQBAL

Thesis submitted in fulfillment of the requirements  
for the degree of  
Doctor of Philosophy

**2011**

## ACKNOWLEDGEMENT

First of all, I would like to express my gratitude to my supervisor Prof. Farook Adam for his kindness, guidance and supervision through my research. Without his support, this project will remain just a dream. I would like to thank Universiti Sains Malaysia for the funds given to conduct this research through RU (1001/PKIMIA/811092, 1001/PKIMIA/814019, 1001/PKIMIA/811092, and 1001/PKIMIA/822100) and USM-RU-PRGS (1001/PKIMIA/832027) grants. I am also pleased to record my gratitude to International Islamic University Malaysia for the sponsorship given to me.

A special gratitude goes to Dr. T. Radhika, Dr. Noor Hana Hanif, Dr. Kassim M. Hello, Dr. Ng Eng-Poh, Dr. Yasodha Sivasodhi, Dr. Sharon Fathinathan, Dr. Melati, Ms. Hanani Yazid, Mr. Tammar, Mr. Muazu, Dr. Ishraga, Dr. Adil, Ms. Jeyashelly, Mrs. Sumiyyah Sabar, fellow friends and lecturers in Heterogeneous Catalysis Laboratory, Inorganic and Organic Section, School of Chemical Sciences, Universiti Sains Malaysia. To my dearest friends, Michelle “Ah So” Teh, Bik, Su, Azrul and Ayie thank you so very much and may God strengthen our friendship till the end of our life.

I would also like to thank all the staff in School of Chemical Sciences, School of Biological Sciences and School of Physics, Universiti Sains Malaysia and those who were directly and indirectly involved in making this thesis possible.

To my parents, wife, brother and sister, I’ll never forget your support and encouragement. Your time, ideas, comments, love and support are appreciated more than you’ll ever know.

**“One can pay back the loan of gold, but one dies forever in debt to those who are kind.”**

## TABLE OF CONTENTS

	<b>Page</b>
<b>ACKNOWLEDGEMENT</b>	ii
<b>TABLES OF CONTENT</b>	iii
<b>LIST OF FIGURES</b>	xi
<b>LIST OF TABLES</b>	xviii
<b>LIST OF SCHEMES</b>	xx
<b>LIST OF SYMBOLS AND ABBREVIATIONS</b>	xxi
<b>LIST OF APPENDIX</b>	xxiv
<b>ABSTRAK</b>	xxv
<b>ABSTRACT</b>	xxvii
<b>CHAPTER ONE- INTRODUCTION</b>	
1.0 The twelve principles of green chemistry	1
1.1 History of catalysis	4
1.2 An overview of oxidation catalysis	5
1.3 Silica	7
1.3.1 Silica in plants	8
1.3.2 Paddy plant	8
1.3.3 Silica in rice husk	9
1.4 Techniques of heterogenization methods of chromium, molybdenum and tungsten	10
1.4.1 Impregnation	11
1.4.2 Direct hydrothermal method	13
1.4.3 Sol-gel method	14
1.5 Benzaldehyde	15

1.5.1	Benzaldehyde from natural sources	16
1.5.2	Chemically synthesized benzaldehyde	17
1.5.2.1	Chlorination of toluene	17
1.5.2.2	Catalytic oxidation of toluene	18
1.5.2.3	Oxidation of styrene	20
1.6	Scope of research	27
1.7	Objectives	28
<b>CHAPTER TWO – EXPERIMENTAL METHODS</b>		
2.0	Raw materials	30
2.1	Extraction and modification of silica from RH	30
2.1.1	Washing and treatment of RH	30
2.1.2	Silica extraction from RH at different pH	31
2.1.3	Chromium, molybdenum and tungsten incorporation into the silica matrix at different pH	31
2.2	Characterization of the catalysts	32
2.2.1	Fourier transform infrared (FT-IR) spectroscopic analysis	33
2.2.2	Nitrogen sorption studies	32
2.2.3	<sup>29</sup> Si MAS NMR spectroscopic analysis	33
2.2.4	Powder X-ray diffraction (XRD) analysis	33
2.2.5	X-ray photoelectron spectroscopic (XPS) analysis	33
2.2.6	Transmission electron microscopy (TEM) analysis	34
2.2.7	Scanning electron microscopy- energy dispersive X-ray (SEM/EDX) spectroscopic analysis	34
2.2.8	Atomic absorption spectroscopic (AAS) analysis	34
2.2.9	Inductively coupled plasma-mass spectroscopic (ICP-MS) analysis	35
2.2.10	UV-Vis diffuse reflectance spectroscopic analysis	35

2.2.11	FT-Raman spectroscopic analysis	36
2.3	Catalytic reactions	36
2.3.1	General reaction procedures	36
2.3.2	Gas chromatography (GC) and Gas chromatography- mass spectrometry (GC-MS) analyses	37

### **CHAPTER THREE- CHARACTERIZATION OF PARENT SILICA SUPPORT PREPARED AT DIFFERENT pH**

3.0	Introduction	39
3.1	Fourier transform infrared (FT-IR) spectroscopic analysis	39
3.2	Nitrogen sorption studies	40
3.3	<sup>29</sup> Si MAS NMR spectroscopic analysis	44
3.4	Powder X-ray diffraction (XRD) analysis	47
3.5	Transmission electron microscopy (TEM) analysis	49
3.6	Scanning electron microscope-energy dispersive X-ray (SEM-EDX) analysis	50
3.7	Summary	52

### **CHAPTER FOUR- CHARACTERIZATION AND CATALYTIC ACTIVITY OF RHCr-3, RHCr-7 AND RHCr-10**

4.0	Introduction	53
4.1	Characterisations of RHCr-3, RHCr-7 and RHCr-10	53
4.1.1	Atomic absorption spectroscopic analysis (AAS)	54
4.1.2	Scanning electron microscope-energy dispersive X- ray (SEM-EDX) analysis	55
4.1.3	Transmission electron microscopy (TEM) analysis	54
4.1.4	UV-Vis diffused reflectance spectroscopic analysis	56
4.1.5	FT-Raman spectroscopic analysis	58
4.1.6	Powder X-ray diffraction (XRD) analysis	60

4.1.7	Fourier transform infrared (FT-IR) spectroscopic analysis	62
4.1.8	Nitrogen sorption studies	63
4.1.9	<sup>29</sup> Si MAS NMR spectroscopic analysis	66
4.2	The liquid phase oxidation of styrene using RHCr-10, RHCr-7 and RHCr-3	68
4.2.1	The effect of catalysts preparation medium on the oxidation of styrene	68
4.2.2	The effect of styrene to H <sub>2</sub> O <sub>2</sub> molar ratio on the oxidation of styrene	71
4.2.3	The effect of temperature on the oxidation of styrene	73
4.2.4	The effect of mass of catalyst in the oxidation of styrene	75
4.2.5	Leaching study	77
4.2.6	Reusability	78
4.2.7	Surface structure of RHCr-3	80
4.3	Re-characterization of used RHCr-3	82
4.3.1	Atomic absorption spectroscopic (AAS) analysis	82
4.3.2	Scanning electron microscope-energy dispersive X-ray (SEM-EDX) analysis	82
4.3.3	Transmission electron microscopy (TEM) analysis	84
4.3.4	UV-Vis diffused reflectance spectroscopic analysis	85
4.3.5	FT-Raman spectroscopic analysis	86
4.3.6	Powder X-ray diffraction (XRD) analysis	87
4.3.7	Fourier transform infrared (FT-IR) spectroscopic analysis	89
4.3.8	Nitrogen sorption studies	90
4.3.9	<sup>29</sup> Si MAS NMR spectroscopic analysis	92
4.3.10	Surface structure of used RHCr-3.	92
4.3.11	Reaction Mechanism	94

4.3.11.1	Reaction mechanism involving Cr <sup>3+</sup> species	95
4.3.11.2	Reaction mechanism involving Cr <sup>6+</sup> species	96
4.3.11.3	Hydroxyl radical catalyzed oxidation of styrene	97
4.4	Summary	101
<b>CHAPTER FIVE- CHARACTERIZATION AND CATALYTIC ACTIVITY OF RHM<sub>o</sub>-3, RHM<sub>o</sub>-7 AND RHM<sub>o</sub>-10</b>		
5.0	Introduction	103
5.1	Characterisations of RHM <sub>o</sub> -3, RHM <sub>o</sub> -7 and RHM <sub>o</sub> -10	103
5.1.1	Atomic absorption spectroscopy (AAS) analysis	103
5.1.2	Scanning electron microscope-energy dispersive X- ray (SEM-EDX) analysis	103
5.1.3	Transmission electron microscopy (TEM) analysis	105
5.1.4	UV-Vis diffused reflectance spectroscopic analysis	106
5.1.5	FT-Raman spectroscopic analysis	108
5.1.6	Powder X-ray diffraction (XRD) analysis	109
5.1.7	Fourier transform infrared (FT-IR) spectroscopic analysis	111
5.1.8	Nitrogen sorption studies	112
5.1.9	<sup>29</sup> Si MAS NMR spectroscopic analysis	115
5.2	The liquid phase oxidation of styrene using RHM <sub>o</sub> -10, RHM <sub>o</sub> -7 and RHM <sub>o</sub> -3	116
5.2.1	The effect of catalysts preparation medium on the oxidation of styrene	116
5.2.2	The effect of styrene to H <sub>2</sub> O <sub>2</sub> molar ratio on the oxidation of styrene	118
5.2.3	The effect of temperature on the oxidation of styrene	120
5.2.4	The effect of mass of catalyst on the oxidation of styrene	122
5.2.5	Leaching study	124
5.2.6	Reusability	125

5.2.7	Surface structure of RHMo-3	127
5.3	Re-characterization of used RHMo-3	129
5.3.1	Atomic absorption spectroscopic (AAS) analysis	129
5.3.2	Scanning electron microscope-energy dispersive X-ray (SEM-EDX) analysis	129
5.3.3	Transmission electron microscopy (TEM) analysis	131
5.3.4	UV-Vis diffused reflectance spectroscopic analysis	132
5.3.5	FT-Raman spectroscopic analysis	133
5.3.6	Powder X-ray diffraction (XRD) analysis	134
5.3.7	Fourier transform infrared (FT-IR) spectroscopic analysis	136
5.3.8	Nitrogen sorption studies	136
5.3.9	<sup>29</sup> Si MAS NMR spectroscopic analysis	139
5.3.10	Surface structure of used RHMo-3	140
5.3.11	Reaction mechanism	141
5.4	Summary	144
	<b>CHAPTER SIX- CHARACTERIZATION AND CATALYTIC ACTIVITY OF RHW-3, RHW-7 AND RHW-10</b>	146
6.0	Introduction	146
6.1	Characterisations of RHW-3, RHW-7 and RHW-10	146
6.1.1	Inductively coupled- mass spectrometry (ICP-MS) analysis	146
6.1.2	Scanning electron microscope-energy dispersive X- ray (SEM-EDX) analysis	147
6.1.3	Transmission electron microscopy (TEM) analysis	148
6.1.4	UV-Vis diffused reflectance spectroscopic analysis	149
6.1.5	FT-Raman spectroscopic analysis	152
6.1.6	Powder X-ray diffraction (XRD) analysis	153

6.1.7	Fourier transform infrared (FT-IR) spectroscopic analysis	155
6.1.8	Nitrogen sorption studies	156
6.1.9	<sup>29</sup> Si MAS NMR spectroscopic analysis	159
6.2	Liquid phase oxidation of styrene using RHW-10, RHW-7 and RHW-3	160
6.2.1	The effect of catalysts preparation medium on the oxidation of styrene	160
6.2.2	The effect of styrene to H <sub>2</sub> O <sub>2</sub> molar ratio on the catalytic activity of RHW-3	162
6.2.3	The effect of temperature on the oxidation of styrene	164
6.2.4	The effect of mass of catalyst in the oxidation of styrene	165
6.2.5	Leaching study	167
6.2.6	Reusability	168
6.2.7	Surface structure of RHW-3	170
6.3	Re-characterization of used RHW-3	172
6.3.1	Inductively coupled- mass spectrometry (ICP-MS) analysis	173
6.3.2	Scanning electron microscope-energy dispersive X-ray (SEM-EDX) analysis	173
6.3.3	Transmission electron microscopy (TEM) analysis	173
6.3.4	UV-Vis diffused reflectance spectroscopic analysis	174
6.3.5	FT-Raman spectroscopic analysis	175
6.3.6	Powder X-ray diffraction (XRD) analysis	176
6.3.7	Fourier transform infrared (FT-IR) spectroscopic analysis	178
6.3.8	Nitrogen sorption studies	179
6.3.9	<sup>29</sup> Si MAS NMR spectroscopic analysis	181
6.3.10	Surface structure of used RHW-3	182
6.3.11	Reaction mechanism	184

6.4 Summary	184
<b>CHAPTER SEVEN- CONCLUSION AND FUTURE OUTLOOKS</b>	
7.1 Conclusion	188
7.2 Future Outlooks	189
<b>References</b>	191
<b>Appendix</b>	204
<b>List of Publications</b>	210
<b>List of Conferences</b>	211

## LIST OF FIGURES

		<b>Page</b>
Fig. 1.1	The images of (a) rice husk and (b) rice husk ash.	9
Fig. 1.2	The structure of amygdalin.	16
Fig. 3.1	The FT-IR spectra of RHSi-10, RHSi-7 and RHSi-3.	40
Fig. 3.2	The nitrogen sorption isotherms of (a) RHSi-10, (b) RHSi-7 and (c) RHSi-3.	41
Fig. 3.3	The pore size distribution of (a) RHSi-10, (b) RHSi-7 and (c) RHSi-3.	42
Fig. 3.4	The silica surface with silicon atoms of various bridging bonds.	44
Fig. 3.5	The $^{29}\text{Si}$ MAS NMR spectra of RHSi-10, RHSi-7 and RHSi-3.	45
Fig. 3.6	The low and high angle XRD diffractograms of RHSi-10, RHSi-7 and RHSi-3.	48
Fig. 3.7	The TEM images of (a) RHSi-10, (b) RHSi-7 and (c) RHSi-3.	49
Fig. 3.8	The SEM images of (a) RHSi-10, (b) RHSi-7 and (c) RHSi-3.	51
Fig. 4.1	The SEM images showing rocky surface of (a) RHCr-10, (b) RHCr-7 and (c) RHCr-3.	54
Fig. 4.2	The TEM images of (a) RHCr-10, (b) RHCr-7 and (c) RHCr-3.	56
Fig. 4.3	Physical appearance of (a) RHCr-10 and (b) RHCr-7 and (c) RHCr-3.	57
Fig. 4.4	The UV-Vis diffuse reflectance spectra of RHCr-10, RHCr-7 and RHCr-3.	58
Fig. 4.5	The Raman spectra of (a) RHCr-10, (b) RHCr-7 and (c) RHCr-3.	59
Fig. 4.6	The low and high angle diffractograms of RHCr-10, RHCr-7 and RHCr-3.	61

Fig. 4.7	The FT-IR spectra of RHCr-10, RHCr-7 and RHCr-3.	62
Fig. 4.8	The nitrogen sorption isotherms of (a) RHCr-10, (b) RHCr-7 and (c) RHCr-3.	63
Fig. 4.9	The pore size distributions of (a) RHCr-10, (b) RHCr-7 and (c) RHCr-3.	65
Fig. 4.10	The $^{29}\text{Si}$ MAS NMR spectra of RHCr-10, RHCr-7 and RHCr-3.	69
Fig. 4.11	Styrene conversion and products selectivity when the reaction was carried out using (a) RHCr-10, (b) RHCr-7 and (c) RHCr-3.	70
Fig. 4.12	The effect of reactant molar ratio on the styrene conversion and products selectivity. The styrene to $\text{H}_2\text{O}_2$ molar ratio was ranged from 1:1 to 1:4.	72
Fig. 4.13	The effect of reaction temperature on the styrene conversion and product selectivity. The reactions were carried out at 303, 338 and 353 K.	74
Fig. 4.14	The effect of different RHCr-3 mass on the styrene conversion and product selectivity. The mass of catalysts used ranged from 25 to 100 mg.	76
Fig. 4.15	Reaction profile showing the styrene conversion percentage during leaching test, blank reaction and RHCr-3. During the leaching RHCr-3 was separated at 30 min after the reaction had begun.	78
Fig. 4.16	Reaction profile showing the conversion of styrene and product selectivity when RHCr-3 was reused.	79
Fig. 4.17	RHCr-3 XPS spectra of (a) Cr 2p, (b) O 1s and (c) Si 2p.	81
Fig. 4.18	The surface structure of RHCr-3 indicating the co-existence of $\text{Cr}^{3+}$ and $\text{Cr}^{6+}$ species.	81
Fig. 4.19	The SEM images of (a) fresh and (b) used RHCr-3.	83
Fig. 4.20	The TEM images of (a) fresh and (b) used RHCr-3.	84
Fig. 4.21	The physical appearance of (a) fresh and (b) used RHCr-3.	85
Fig. 4.22	The UV-Vis diffuse reflectance spectra of fresh and used RHCr-3.	86

Fig. 4.23	The FT-Raman spectra of (a) fresh and (b) used RHCr-3.	87
Fig. 4.24	The low and high angle XRD diffractograms of fresh and used RHCr-3.	88
Fig. 4.25	The FT-IR spectra showing the comparison between fresh and used RHCr-3.	89
Fig. 4.26	The nitrogen sorption isotherms of fresh and used RHCr-3.	90
Fig. 4.27	The pore size distribution of fresh and used RHCr-3.	91
Fig. 4.28	The $^{29}\text{Si}$ MAS NMR spectra of used and fresh RHCr-3.	93
Fig. 4.29	The XPS spectra of used RHCr-3 (a) Cr 2p, (b) O1s and (c) Si2p.	93
Fig. 4.30	Surface structure of used RHCr-3 indicating the presence of $\text{Cr}^{3+}$ and $\text{Cr}^{6+}$ species.	94
Fig. 5.1	The SEM images of (a) RHMo-10, (b) RHMo-7 and (c) RHMo-3 showing the spherical surface on rocky particles.	104
Fig. 5.2	The TEM images of (a) RHMo-10, (b) RHMo-7, and (c) RHMo-3.	105
Fig. 5.3	The physical appearance of (a) RHMo-10, (b) RHMo-7 and (c) RHMo-3.	106
Fig. 5.4	The UV-Vis diffuse reflectance spectra of RHMo-10, RHMo-7 and RHMo-3.	107
Fig. 5.5	The FT-Raman spectra of (a) RHMo-10, (b) RHMo-7 and (c) RHMo-3.	108
Fig. 5.6	The low and high angle XRD diffractograms of RHMo-10, RHMo-7 and RHMo-3.	110
Fig. 5.7	The FT-IR spectra of RHMo-10, RHMo-7 and RHMo-3.	111
Fig. 5.8	The nitrogen sorption isotherms of (a) RHMo-10, (b) RHMo-7 and (c) RHMo-3.	112
Fig. 5.9	The pore size distributions of (a) RHMo-10, (b) RHMo-7 and (c) RHMo-3.	114
Fig. 5.10	The $^{29}\text{Si}$ MAS NMR spectra of (a) RHMo-10, (b) RHMo-7 and (c) RHMo-3.	115

Fig. 5.11	The styrene conversion and products selectivity when the reaction was carried out using (a) RHMo-10, (b) RHMo-7 and (c) RHMo-3 as the catalyst.	117
Fig. 5.12	The effect of styrene: hydrogen peroxide molar ratio on the styrene conversion and product selectivity. The molar ratio used was ranged from 1:1 to 1:4.	119
Fig. 5.13	The effect of reaction temperature on the styrene conversion and product selectivity of RHMo-3. The reactions were carried out at (a) 303 K, (b)338 K and (c) 353 K.	121
Fig. 5.14	The influence of RHMo-3 mass on the styrene conversion and product selectivity.	123
Fig. 5.15	Percentages of conversion of styrene during leaching test as compared to using fresh RHMo-3, blank reaction (without catalyst) and RHSi-3. During leaching test, the catalyst was removed at 30 min and the reaction allowed to continue to completion in 6 h.	125
Fig. 5.16	Styrene conversion and product selectivity when RHMo-3 was used repeatedly.	126
Fig. 5.17	The XPS spectra of RHMo-3 of (a) Mo 3d, (b) O1s and (c) Si 2p.	127
Fig. 5.18	The possible structure of RHMo-3 based on XPS, <sup>29</sup> Si MAS NMR, UV–Vis diffuse reflectance and FT- IR spectroscopy analyses.	127
Fig. 5.19	The SEM images of (a) fresh and (b) used RHMo-3.	130
Fig. 5.20	The TEM images of (a) fresh and (b) used RHMo-3 showing dark spots due to the agglomeration of particles.	131
Fig. 5.21	The physical appearance of RHMo-3 (a) before and (b) after being used as a catalyst in the oxidation of styrene.	132
Fig. 5.22	The UV-Vis diffuse reflectance spectra of fresh and used RHMo-3.	133
Fig. 5.23	The FT-Raman spectra of fresh and used RHMo-3.	134
Fig. 5.24	The low and high angle XRD diffractograms of fresh and used RHMo-3.	135
Fig. 5.25	The FT-IR spectra of fresh and used RHMo-3.	136

Fig. 5.26	The nitrogen sorption isotherms of (a) fresh and (b) used RHM <sub>o</sub> -3.	137
Fig. 5.27	The BET nitrogen sorption parameters of fresh and used RHM <sub>o</sub> -3.	138
Fig. 5.28	The <sup>29</sup> Si MAS NMR spectra of fresh and used RHM <sub>o</sub> -3.	139
Fig. 5.29	Diagram showing the formation of silanol bond.	140
Fig. 5.30	Used RHM <sub>o</sub> -3 XPS spectra of (a) Mo 3d, (b) O1s and (c) Si 2p.	141
Fig. 5.31	Proposed surface structure of RHM <sub>o</sub> -3 after catalytic activity.	141
Fig. 6.1	The SEM images of (a) RHW-10, (b) RHW-7 and (c) RHW-3. Bright spot can be seen in the image of RHW-7 and RHW-3.	148
Fig. 6.2	The TEM images of (a) RHW-10, (b) RHW-7 and (c) RHW-3.	149
Fig. 6.3	The physical appearance of (a) RHW-10, (b) RHW-7 and (c) RHW-3.	150
Fig. 6.4	The UV-Vis diffuse reflectance spectra of (a) RHW-10, (b) RHW-7 and (c) RHW-3	151
Fig. 6.5	The FT-Raman spectra of (a) RHW-10, (b) RHW-7 and (c) RHW-3.	152
Fig. 6.6	The low and high angle XRD diffractograms of RHW-10, RHW-7 and RHW-3.	154
Fig. 6.7	The FT-IR spectra of RHW-10, RHW-7 and RHW-3.	155
Fig. 6.8	The nitrogen sorption isotherms of (a) RHW-10, (b) RHW-7 and (c) RHW-3.	156
Fig. 6.9	The pore size distribution of (a) RHW-10, (b) RHW-7 and (c) RHW-3.	158
Fig. 6.10	The <sup>29</sup> Si MAS NMR spectra of (a) RHW-10, (b) RHW-7 and (c) RHW-3.	159
Fig. 6.11	The percent conversion and product selectivity over tungsten-silica catalysts prepared at different pH.	161

Fig. 6.12	The conversion of styrene and product selectivity at different styrene: hydrogen peroxide molar ratio.	163
Fig. 6.13	The effect of reaction temperature on the percentage of conversion of styrene and product selectivity	164
Fig. 6.14	Styrene conversion and product selectivity obtained using different mass of RHW-3.	166
Fig. 6.15	The reaction profile showing the comparison between fresh RHW-3, leaching test, blank and RHSi-3. The catalyst was separated at 30 min in the leaching test.	168
Fig. 6.16:	Styrene conversion and product distribution when RHW-3 was reused. The reaction was carried out under optimum conditions.	169
Fig. 6.17	The RHW-3 XPS spectra of (a) W4f, (b) O1s and (c) Si 2p.	171
Fig. 6.18	The proposed active surface structure of RHW-3.	171
Fig. 6.19	The SEM images of (a) fresh and (b) used RHW-3.	173
Fig. 6.20	The TEM images of (a) fresh and (b) used RHW-3.	173
Fig. 6.21	The physical appearance of (a) fresh RHW-3 and (b) used RHW-3. The yellow colour of the catalyst is an indication of the existence of crystalline WO <sub>3</sub> in RHW-3.	174
Fig. 6.22	The UV-Vis diffuse reflectance spectra of used and fresh RHW-3. Both spectra indicate the presence of similar tungsten species.	175
Fig. 6.23	The FT-Raman spectra of fresh and used RHW-3.	176
Fig. 6.24	The low and high angle XRD diffractograms of fresh and used RHW-3.	177
Fig. 6.25	The FT-IR spectra of used and fresh RHW-3.	178
Fig. 6.26	The type IV isotherm indicating H2 hysteresis loop of (a) fresh and (b) used RHW-3.	179
Fig. 6.27	The pore size distribution of fresh and used RHW-3.	180
Fig. 6.28	The <sup>29</sup> Si MAS NMR spectra of fresh and used RHW-3.	181
Fig. 6.29	The used RHW-3 XPS spectra of (a) W4f, (b) O1s and (c) Si 2p.	183

Fig. 6.30 The proposed surface structure of RHW-3 after catalytic activity.

183

## LIST OF TABLES

		<b>Page</b>
Table 2.1	GC and GC-MS conditions for the separation and identification of the oxidation of styrene products.	38
Table 3.1	The nitrogen sorption analysis data for RHSi-10, RHSi-7 and RHSi-3.	43
Table 3.2	The elements detected by EDX in RHSi-10, RHSi-7 and RHSi-3.	51
Table 4.1	Elements detected by EDX analysis in RHCr-10, RHCr-7 and RHCr-3. Bulk chromium percentage determined by AAS analysis is also included.	55
Table 4.2	Comparison between RHSi-10, RHSi-7 and RHSi-3 and RHCr-10, RHCr-7 and RHCr-3 nitrogen sorption properties.	65
Table 4.3	Comparison between elements found in fresh RHCr-3 and used RHCr-3. Bulk chromium percentage determined by AAS analysis is also included.	83
Table 4.4	The nitrogen sorption properties comparison between fresh and used RHCr-3.	91
Table 5.1	The elements detected by EDX analysis in RHMo-10, RHMo-7 and RHMo-3 and bulk molybdenum percentage detected by AAS.	104
Table 5.2	The nitrogen sorption properties of RHMo-10, RHMo-7 and RHMo-3 are shown together with the nitrogen sorption properties of RHSi-10, RHSi-7 and RHSi-3 given for comparison.	114
Table 5.3	The elements detected by EDX analysis in fresh and used RHMo-3. Bulk molybdenum percentage detected by AAS analysis is also included.	130
Table 5.4	The BET nitrogen sorption parameters of fresh and used RHMo-3.	138
Table 6.1	The elements detected by EDX in RHW-10, RHW-7 and RHW-3. Bulk tungsten percentage detected by ICP-MS is also included.	147
Table 6.2	The parameters of nitrogen sorption surface analysis for RHSi-10, RHSi-7, RHSi-3, RHW-10, RHW-7 and RHW-3.	159

Table 6.3	Elements detected by EDX analysis of fresh and used RHW-3. Bulk tungsten percentage detected by ICP-MS is also included.	172
Table 6.4	The nitrogen sorption surface analysis parameters of fresh and used RHW-3.	180

## LIST OF SCHEMES

		<b>Page</b>
Scheme 1.1	Benzaldehyde preparation route from cinnamaldehyde.	17
Scheme 1.2	Aerobic oxidation of toluene catalyzed by Mn(III)TPP/CTS catalyst.	18
Scheme 1.3	Products obtained from the oxidation of styrene using hydrogen peroxide.	21
Scheme 1.4	Reaction mechanism involving the formation of transient vanadyl diradical species and vanadium-peroxy-styrene intermediate.	25
Scheme 1.5	Reaction mechanism of oxidation of styrene involving peroxo-metal complex reaction.	26
Scheme 1.6	Peroxometalocycle-catalyzed oxidation of styrene.	26
Scheme 1.7	Formation of benzaldehyde from the cleavage of hydroperoxystyrene intermediate.	27
Scheme 4.1	The interaction between (a) chromium(III) hydroperoxide and (b) chromyl diradical species leading to the formation of styrene oxide, benzaldehyde, formaldehyde and water.	95
Scheme 4.2	The formation of chromium inorganic peracid upon interaction with hydrogen peroxide. The image also shows the formation of benzaldehyde and formaldehyde.	99
Scheme 4.3	The reaction mechanism involving the formation of chromium inorganic peracid and Cr <sup>6+</sup> redox system.	100
Scheme 5.1	The proposed reaction mechanism for the oxidation of styrene using RHMo-3.	143
Scheme 6.1	The proposed mechanism for the formation of Bza using RHW-3 as catalyst.	187

## LIST OF SYMBOLS AND ABBREVIATIONS

1-POH	1-phenylethanol
3D	3 dimensions
Å	Angstrom
AAS	Atomic absorption spectroscopy
Ace	Acetophenone
a.u	arbitrary unit
BA	Benzoic acid
BJH	Barret, Joyner and Halenda
Bza	Benzaldehyde
ccg <sup>-1</sup>	cubic centimetre per gram
CTAB	Cetyltrimethylammonium bromide
DMF	Dimethylformamide
EDX	Energy dispersive X-ray spectroscopy
eV	electron volt
Fig	Figure
FT-IR	Fourier transform infrared
g	gram
GC	Gas chromatography
GC-MS	Gas chromatography-mass spectrometry
h	Hour
ICP-MS	Inductively coupled plasma-mass spectrometry
IUPAC	The International Union of Pure and Applied Chemistry
K	Kelvin (absolute temperature unit)

kV	kilovolt
M	Molar concentration
$\text{m}^2 \text{g}^{-1}$	meter squared per gram
$\text{m}^3 \text{h}^{-1}$	meter cube per hour
mA	milliampere
MAS NMR	Magic angle spinning nuclear magnetic resonance
mg	milligram
mm Hg	millimeters of mercury
mmol	millimole
min	minutes
MPa	megapascals
PhAA	Phenylacetaldehyde
Pxal	Phenylglyoxal
RH	Rice husk
RHA	Rice husk ash
RHCr-10	Chromium incorporated silica at pH 10
RHCr-3	Chromium incorporated silica at pH 3
RHCr-7	Chromium incorporated silica at pH 7
RHMo-10	Molybdenum incorporated silica at pH 10
RHMo-10	Molybdenum incorporated silica at pH 10
RHMo-10	Molybdenum incorporated silica at pH 10
RHMo-3	Molybdenum incorporated silica at pH 3
RHMo-7	Molybdenum incorporated silica at pH 7
RHSi-10	Silica extracted from rice husk and precipitated at pH 10
RHSi-3	Silica extracted from rice husk and precipitated at pH 3

RHSi-7	Silica extracted from rice husk and precipitated at pH 7
RHW-10	Tungsten incorporated silica at pH 10
RHW-3	Tungsten incorporated silica at pH 3
RHW-7	Tungsten incorporated silica at pH 7
s	Second
SBA	Santa Barbara Amorphous
SEM	Scanning electron microscopy
Si-OH	Silanol
Si-O-Si	Siloxane
StO	Styrene oxide
Stycol	Styrene glycol
T	Tesla
TEM	Transmission electron microscopy
TEOS	Tetra ethyl orthosilicate
TMOS	Tetra methyl orthosilicate
TMS	Tetramethylsilane
TON	Turn over number
TPR	Temperature-Programmed Reduction
XPS	X-ray photoelectron spectroscopy
XRD	Powder X-ray diffractometry

## LIST OF APPENDIX

### Appendix A

	<b>Page</b>
A1: Liquid phase oxidation of styrene reaction mixture gas chromatograph.	205
A2: Mass spectra of <i>m</i> -xylene and styrene.	206
A3: Mass spectra of benzaldehyde (Bza) and styrene oxide (StO).	207
A4: Mass spectra of phenylacetaldehyde (PhAA) and acetophenone (Ace).	208
A5: Mass spectra of 1-phenylethanol (1-POH) and phenylglyoxal (Pxl).	209
A6: Mass spectra of benzoic acid (BA) and styrene glycol (Stycol).	210

# MANGKIN HETEROGEN DARI SEKAM PADI TERUBAHSUAI DENGAN KROMIUM, MOLIBDINUM DAN TUNGSTEN: SINTESIS, PENCIRIAN DAN KEGUNAANNYA DI DALAM PENGOKSIDAAN STIRINA

## Abstrak

Satu siri mangkin kromium, molibdinum dan tungsten digabungkan dengan silika yang diekstrak dari sekam padi melalui kaedah pengekstrakan pelarut dan teknik sol-gel pada pH 10, pH 7 dan pH 3. Tindak balas pengoksidaan stirina dalam fasa cecair digunakan sebagai medium untuk mengkaji kebolehan mengoksida mangkin-mangkin tersebut. Penggabungan kromium ke dalam matriks silika telah menghasilkan mangkin amorfus yang dilabel sebagai RHCr-10, RHCr-7 and RHCr-3. Luas permukaan RHCr-3 ( $564 \text{ m}^2 \text{ g}^{-1}$ ) adalah yang tertinggi manakala kandungan kromium pula adalah yang terendah (2.3 w/w %). RHCr-3 mempunyai struktur dan kebolehan memangkin yang lebih baik berbanding RHCr-10 dan RHCr-7. Sebanyak 99.9 % stirina telah dioksidakan dengan 63.1 % selektiviti terhadap benzaldehid. Keasidan medium tindak balas, luas permukaan yang tinggi dan kewujudan spesis  $\text{Cr}^{3+}$  dan  $\text{Cr}^{6+}$  telah meningkatkan keupayaan memangkin RHCr-3. Pencirian semula RHCr-3 yang telah digunakan menunjukkan sedikit perubahan dalam jumlah kromium, luas permukaan dan isipadu liang akibat kehilangan tapak aktif kromium. Tindak balas pengoksidaan stirena menggunakan RHCr-3 dijangka dimangkin oleh spesis  $\text{Cr}^{3+}$  dan  $\text{Cr}^{6+}$ . Penggabungan molibdinum ke dalam matriks silika telah menghasilkan mangkin amorfus berlabel RHMo-10, RHMo-7 dan RHMo-3. Pencirian fiziko-kimia mangkin-mangkin ini menunjukkan spesis molibdenum tertumpu pada permukaan penyokong. Peratus tertinggi molibdinum ditemui dalam RHMo-3 (7.6 w/w %) manakala luas permukaan RHMo-3 adalah yang terendah ( $445 \text{ m}^2 \text{ g}^{-1}$ ). Kewujudan spesis  $\text{Mo}^{5+}$  dan  $\text{Mo}^{6+}$  telah meningkatkan keaktifan RHMo-3. Sebanyak 82.2 % stirina telah dioksidakan ke produk dengan 82.8 %

selektiviti terhadap benzaldehid. RHMo-3 kehilangan sejumlah besar sifat pemangkinnya akibat kekurangan tapak aktif molibdenum. Pencirian semula RHMo-3 yang telah digunakan menunjukkan perubahan dalam luas permukaan, isipadu, saiz liang dan permukaan tapak aktif. Tindak balas pengoksidaan dijangka dimungkinkan oleh perantara seperti asid permolibdik. Penggabungan tungsten ke dalam matriks silika telah menghasilkan mangkin amorfus RHW-10 dan RHW-7 dan mangkin separa-kristal RHW-3. Pelbagai spesis tungsten ditemui pada permukaan mangkin tersebut. Peratusan tungsten yang tinggi telah meningkatkan potensi memangkin RHW-3 (7.1 w/w %). Sebanyak 61.9 % stirina telah dioksidakan dengan 100 % selektiviti terhadap benzaldehid. Kehilangan tapak aktif spesis tungsten telah menyebabkan perubahan kecil dalam peratusan tungsten, luas permukaan, isipadu liang, sistem liang dan tapak permukaan aktifnya. Tindak balas pengoksidaan dijangka dimungkinkan oleh perantara seperti asid pertungstik. Turutan kebolehan mangkin tersebut dalam mengoksida stirina adalah seperti berikut: RHCr-3 > RHMo-3 > RHW-3 manakala turutan mengikut keselektifan terhadap benzaldehid adalah seperti berikut: RHW-3 > RHMo-3 > RHCr-3.

# HETEROGENEOUS CATALYSTS FROM RICE HUSK MODIFIED WITH CHROMIUM, MOLYBDENUM AND TUNGSTEN: SYNTHESIS, CHARACTERIZATION AND APPLICATION IN STYRENE OXIDATION

## Abstract

A series of chromium, molybdenum and tungsten incorporated silica extracted from rice husk were prepared at pH 10, pH 7 and pH 3 media using solvent extraction method and sol-gel technique. Liquid phase oxidation of styrene using hydrogen peroxide as oxidant was used as a probe to test their catalytic potential. The incorporation of chromium into the silica matrix resulted in amorphous catalysts labeled RHCr-10, RHCr-7 and RHCr-3. RHCr-3 has the highest surface area ( $564 \text{ m}^2 \text{ g}^{-1}$ ) but lowest chromium loading (2.3 w/w %). RHCr-3 showed better structural and catalytic properties compared to RHCr-7 and RHCr-10. About 99.9 % of styrene was successfully oxidized with 63.1 % selectivity towards benzaldehyde. Acidic pH of the reaction medium, higher surface area and the existence of  $\text{Cr}^{3+}$  and  $\text{Cr}^{6+}$  were predicted to increase the catalytic activity of RHCr-3. Re-characterization of used RHCr-3 showed slight changes in chromium loading, surface area and pore volume due to leaching. RHCr-3 is proposed to catalyze the reaction via  $\text{Cr}^{3+}$  and  $\text{Cr}^{6+}$  species. The incorporation of molybdenum into the silica matrix resulted in amorphous catalysts labeled as RHMo-10, RHMo-7 and RHMo-3. Physico-chemical characterization on these catalysts indicates that molybdenum species prefer to be on the surface of the support. Highest molybdenum percentage was found in RHMo-3 (7.6 w/w %) whereas the surface area of RHMo-3 was the lowest ( $445 \text{ m}^2 \text{ g}^{-1}$ ). The existence of  $\text{Mo}^{5+}$  and  $\text{Mo}^{6+}$  species had increased the activity of RHMo-3. About 82.2 % of styrene was oxidized and benzaldehyde selectivity was 82.8 %. RHMo-3 faced massive loss in its catalytic activity due to leaching. Re-characterization of used RHMo-3 indicates rapid changes in its surface area, pore volume, pore size

distribution and surface active sites. The oxidation reaction is proposed to proceed via permolybdic acid like intermediate. Tungsten incorporation into the silica matrix resulted in amorphous RHW-10 and RHW-7 and semi-crystalline RHW-3 catalysts. Different kind of tungsten species were detected on the surface of the catalysts. Higher tungsten percentage in RHW-3 (7.1 % w/w) had increased its catalytic potential. About 61.9 % of styrene was oxidized with 100 % selectivity towards Bza. Leaching had caused slight changes in the surface area, pore volume, pore size distribution and its surface active sites. The reaction was predicted to be catalyzed by pertungstic acid like intermediate. The order of the catalysts in oxidizing styrene is  $\text{RHCr-3} > \text{RHMo-3} > \text{RHW-3}$  whereas the order of the catalysts in terms of selectivity towards benzaldehyde is  $\text{RHW-3} > \text{RHMo-3} > \text{RHCr-3}$ .

## CHAPTER ONE

### INTRODUCTION

#### 1.0 The twelve principles of green chemistry

Green Chemistry is not a new branch of chemistry but it is an approach in carrying out chemistry in a sustainable manner (Mike, 2010). The definition of green chemistry was coined in the early 1990's by Anastas and Warner (1998) from the US Environmental Protection Agency (EPA):

*“To promote chemical technologies that reduce or eliminate the use or generation of the hazardous substances in the design, manufacture and use of chemical products.”*

The development of green chemistry can be achieved by designing and conducting experiments according to the twelve principles listed by Anastas and Warner (1998). The principles are as follows:

##### i. **Prevention**

It is better to prevent waste than to generate or dispose of waste after it has been created.

##### ii. **Atom economy**

Synthetic methods should be designed to maximize the incorporation of all materials used in the process into the final product.

iii. **Less hazardous chemical syntheses**

Synthetic methods should be designed to use and generate substances that possess little or no harm to human health and the environment wherever practicable.

iv. **Designing safer chemicals**

Chemical products should be designed to effect their desired function without harming environment.

v. **Safer solvents and auxiliaries**

The use of substances such as solvents, separation agents, etc should be minimized or avoided wherever possible.

vi. **Design for energy efficiency**

Energy consumption in chemical processes should be minimized due to their impacts on environmental and economy. If possible, chemical processes should be conducted at ambient temperature and pressure.

vii. **Use of renewable feedstock**

A raw material or feedstock should be renewable rather than depleting whenever technically and economically practicable.

viii. **Reduce derivatives**

Unnecessary derivatization (use of blocking groups, protection/deprotection, temporary modification of physical/chemical processes) should be minimized or avoided if possible.

ix. **Catalysis**

Catalytic reagents (as selective as possible) are better than stoichiometric reagents.

x. **Design for degeneration**

Chemical products should be designed so that at the end of their function they break down into harmless degradable products.

xi. **Real time analysis for pollution prevention**

Analytical methodologies need to be up-graded to allow for real-time, in-process monitoring and control prior to the formation of hazardous substances.

xii. **Inherently safer chemistry for accident prevention**

Substances and the form of a substance used in a chemical process should be chosen to minimize the potential threats for chemical accidents, including releases, explosions, and fires.

## 1.1 History of catalysis

In 1836, Berzelius published a paper for the Stockholm Academy of Sciences reviewing a number of earlier findings on chemical change in both homogeneous and heterogeneous systems and rationally co-ordinated these findings leading to the introduction of the concept of catalysis. He defined catalysis as reactions that are accelerated by substances that remain unchanged after the reaction. He wrote (John, 2010)

*“It is, then, proved that several simple or compound bodies, soluble and insoluble, have the property of exercising on other bodies an action very different from chemical affinity. By means of this action they produce, in these bodies, decompositions of their elements and different recombinations of these same elements to which they remain indifferent.”*

Catalysts have been used for more than 100 years in fermentation process, conversion of ammonia to nitric acid catalytic hydrogenation, etc. It is estimated that 80 % of all compounds produced today in chemical and pharmaceuticals industries involve at least one catalytic step in their synthesis. Catalysis have been divided into three major categories; homogeneous, heterogeneous and biocatalysis or enzymatic catalysis. In homogeneous catalysis, the catalysts and reactants are in the same phase while in heterogeneous catalysis, catalysts and reactants exist in different phases. The third group, biocatalysis or enzymatic catalysis, is designed based on substrate-active interaction (Miralles, 2009). However, only homogeneous and heterogeneous catalysis received most attention compared to biocatalysis or enzymatic catalysis. According to the Fredonia Group, the world demand on catalysts is estimated to increase up to \$ 16.3 billion by the year 2012 (Armor, 2011; Radhika, 2005). Catalysts-assisted oxidation reaction is one of the most studied chemical reactions.

## 1.2 An overview of oxidation catalysis

For decades, oxidation of hydrocarbon has gained great interest from both academia and industries due to its valuable products such as epoxide, aldehyde, ketone, etc. These products have become important commodities in the production of epoxy resins cosmetics, surface coating, sweeteners, perfume, drugs, etc (Misnon, 2007).

Transition metals have special characteristics in efficiently oxidizing saturated alkenes. Chromium, molybdenum and tungsten are among transition metals that have been widely used in the alkene oxidation. Capability of transition metals in catalyzing a reaction is associated with their partially filled *d*-orbitals. Transfer of electrons is believed to take place from the adsorbed species (reactants) to these partially empty *d*-orbitals on the surface of these transition metals (Clark, 1953).

Chromium (Cr) with the ground state electronic configuration  $1s^2 2s^2 2p^6 3s^2 3p^6 4s^1 3d^5$  exists in all oxidation states from -2 to +6. Chromium behaves as a reducing agent in its lowest oxidation states and as a strongly oxidizing agent in its highest oxidation states. For over a century, chromic acid was a popular oxidation reagent used in organic chemistry. However, recent advancement in catalysis research opened possibilities of creating different kinds of chromium-based catalysts.

The ground state electronic configuration for molybdenum (Mo) is  $1s^2 2s^2 2p^6 3s^2 3p^6 3d^{10} 4s^2 4p^6 4d^5 5s^1$ . Molybdenum species too exist from -2 to +6 oxidation states. Among them, soluble  $Mo^{6+}$  species was favored for its versatility in the oxidation processes (Buffon & Schuchardt, 2003). One good example portrayed by molybdenum as an effective catalyst is in the Halcon process for the industrial

manufacturing of propylene oxide (Qihua et al., 2003). Since then, soluble molybdenum complex with carboxylic acids, ketones, alcohols, glycols, amines, thiols, heterocyclic compounds, etc have been widely synthesized and applied in the oxidation of various types of alkene.

The electronic configuration of tungsten at its ground state is  $1s^2 2s^2 2p^6 3s^2 3p^6 4s^2 3d^{10} 4p^6 5s^2 4d^{10} 5p^6 6s^2 4f^{14} 5d^4$ . Tungsten has similar chemical properties with molybdenum compared to chromium. Oxidation states of tungsten also exist from -2 to +6. Tungsten is a good oxidizing catalyst when coupled with hydrogen peroxide. Tungsten-hydrogen peroxide combinations have been effectively used in the epoxidation of maleic, fumaric and crotonic acid (Bäckvall, 2004).

Even though homogeneous catalysis is unbeaten by its counterpart in terms of catalytic activity and selectivity, it is still not favored in industries. The ratio between heterogeneous to homogeneous catalysis applied in industries is 75:25 (Cornils & Herrmann, 2003).

Homogeneous chromium, molybdenum and tungsten catalysts are often associated with disadvantages such as corrosion, toxicity, handling problem, difficulty in recovery and separation of the catalysts from the reaction mixture and low turnover number (Sheldon et al., 2000; Kotov & Balbolov, 2001; Melero et al., 2007). Therefore, there has been considerable amount of efforts taken to heterogenize these catalysts.

The discovery of ordered mesoporous materials by the researchers from the Mobil Oil Company had initiated an intensive research effort resulting in more than 3000 publications especially in mesoporous materials made of silica. The inertness of silica in catalyzing reactions aided with the ease of structural tailoring has made

silica a good inorganic material to support transition metals (Tuel, 1999; Xinhong & Xiaolai, 2007).

### **1.3 Silica**

Silicon is the second most abundant elements found on the earth's crust after oxygen. It exists as silicon dioxide ( $\text{SiO}_2$ ) when it combines with oxygen or as silicates when it combines with oxygen and other elements. Silicon compounds have been founds in rocks, sand, clays, soils, water, plants and even in animals.

In nature, silica exists in an amorphous and crystalline form. The latter being the major form. The most commonly found crystalline silica is in the form of quartz, cristobolite and tridymite. Amorphous silica is found in the form of fibers, sheets, sols, gels and powders. Compared to crystalline silica, amorphous silica are more favourable to adsorption and catalysis studies. Amorphous silica can easily be tailored to specific properties compared to its counterpart (Iller, 1979; Adil, 2008).

The major precursors used in most research area related to silica are the expensive alkoxysilane compounds such as tetra ethyl orthosilicate (TEOS) and tetra methyl orthosilicate (TMSO) (Adil, 2008). Study done on the toxicity of tetra ethyl orthosilicate (TEOS) by Nashima et al. (1998) revealed that acute exposure can lead to death. Search for a safer and cheaper source of silica precursor has become more demanding due to the cost, health and environment. Naturally occurring silica in plants and their waste can provide an alternative source for a cheaper and safer source of silica.

### **1.3.1 Silica in plants**

Silica in plants can be found in the concentration range of 0.1 – 10 %. In plants, silica is usually found in the form of phytoliths or hydrogen bonded to cellulose molecules in the cell wall as a silica gel,  $\text{SiO}_2 \cdot n\text{H}_2\text{O}$ . The concentration of silica in plants may equal or exceed other macronutrients. However, the ability of plants to accumulate silica varies from one species to another (Currie & Perry, 2007).

Silica absorbed is deposited in cell lumen, cell walls and intercellular spaces. Accumulation of silica also takes place in the external layers below and above the cuticles of leaves, roots and inflorescence bracts of cereal such as rice and wheat (Kraska, 2005).

### **1.3.2 Paddy plant**

Rice has been a staple food source for most part of this world especially in Asia. About 92 % of world rice production and 90% of global rice consumption originates from Asia (Maclean et al., 2002). Paddy plant has been identified as one of the most efficient plant in accumulating silica even from silica deficient soil.

The presence of silica is important for the growth of paddy. Silica deficiency in paddy plant has been identified to increase the likelihood of rice to blast (*Magnaporthe grisea*), leaf blight (*Xanthomonas oryzae pv. oryzae*), brown spot (*Cochliobolus miyabeanus*), stem rot (*Magnaporthe salvinii*), scald (*Monographella albescens*), and grain discoloration. The existence of silica in the plant cell will make the tissues less digestible by chewing insect such as stem borer (*Chilo suppressalis*) (Rodrigues et al., 2003).

### 1.3.3 Silica in rice husk

Out of 600 million tonnes of rice produced worldwide each year, 20 % constitutes the rice husk (RH). Rice husk is composed of 20 % ash, 38 % cellulose, 22 % lignin, 18 % pentose and 2 % other organic moieties (Adam et al., 2006). The purity of silica obtained from RH is ca. 92-95 % which can be further purified to 99.9 % (Ikram & Akhtar, 1988; Radhika & Sugunan, 2006). In most developing countries, the mass production of rice husk creates disposal problems. Very few attempts have been made by researchers from various fields to transform this agricultural waste into more valuable end products. Normally the RH will be incinerated as a way of disposal. Incineration of rice husk will produce rice husk ash (RHA) and liberates fumes and toxic organic gases leading to serious environmental and health problems (Kumagai et al., 2008). The images of RH and RHA are shown in Fig.1(a) and (b).



Fig. 1.1: The images of (a) rice husk and (b) rice husk ash.

Rice husk ash obtained by burning rice husk at elevated temperatures has gained attention in recent years. RHA has been used as an insulator in the production of high quality flat steel due to its high thermal conductivity and melting point. RHA had also been used in the production of low cost building blocks and the

production of high quality cement. RHA is added to enhance the cement properties. RHA-containing Portland cement has higher compressive strength (Bondioli et al., 2007). Rice husks have also been used as a fuel in boiler furnace and as an adsorbent (Srivastava et al., 2006). The presence of silica inside rice husk limits their usage as adhesive due to weak interaction between particle and matrix (Ndazi et al., 2007).

RHA has been used as a silica precursor to synthesize transition metal supported heterogeneous catalysts such as MCM-41 (Michorczyk, et al., 2008; Klimanova et al., 2003), SBA-15(Wang et al., 2009; Balcar et al., 2009), MCM-48, etc (Wang et al., 2009; Zhao et al., 2010).

Research by Adam and Andas (2007), Adam and Cheah (2008) and Adam et al. (2009) has discovered a more environmentally friendly and cost effective method to obtain silica from rice husk without incinerating the husk. They managed to extract silica from the rice husk in the form of sodium silicate solution via solvent extraction at room temperature and atmospheric pressure. Even though the heterogeneous catalysts prepared via solvent extraction route were in amorphous form, these catalysts showed remarkable catalytic activity in the benzylation and oxidation reactions.

#### **1.4 Techniques of heterogenization of chromium, molybdenum and tungsten**

Various methods have been used to prepare stable chromium, molybdenum and tungsten heterogeneous catalysts on silica with unique properties. Depending on the incorporation method and conditions applied, the surface properties, nature of adsorption sites and active sites were expected to vary. Chromium, molybdenum and tungsten-silica heterogeneous catalysts are mostly prepared by wet chemistry techniques such as impregnation, direct hydrothermal synthesis and sol-gel method.

These techniques are known to give solids with large surface area and high porosity in the range of meso and macropores. Some examples of catalysts preparation methods and their effect on the catalytic activity are discussed below.

#### **1.4.1 Impregnation**

Impregnation is widely used in the catalysts manufacturing industry for practical and economic reasons. In this process, a solution containing metal salt precursor is brought into contact with the support which was prepared separately (Goldwasser et al., 1995). The metal salt precursor migrates from the solution into the silica matrix by capillary action. The effectiveness of impregnation method depends largely on the concentration of the impregnating solution, solution volume, impregnation time, and the support textural characteristics (Pizzio, et al., 2001). However, the tendency of metal or metal oxide to agglomerate on the outer surface and the difficulties in controlling particle growth are high. Higher loading of metal is difficult to achieve under this method. The possibility of pores being clogged is also high (Köhn et al., 2001; Köhn et al., 2003; Cannas et al., 2004).

Zhang et al. (2008) compared the properties of Cr-SBA-15 and CrO<sub>x</sub>/SBA-15, respectively, prepared using hydrothermal method and impregnation method. Based on the H<sub>2</sub>-TPR analysis, they reported that high temperature was required to reduce Cr<sup>6+</sup> species found in Cr-SBA-15 compared to CrO<sub>x</sub>/SBA-15 due to the greater dispersion of chromium species in Cr-SBA-15. Although, chromium species in CrO<sub>x</sub>/SBA-15 can be reduced at lower temperature, the quality of the catalyst in terms of surface area and pore volume decreased compared to the hydrothermally prepared Cr-SBA-15. However, the authors did not test the ability of the catalysts in any catalytic reactions.

Bakala et al. (2007) compared a series of silica supported molybdenum(VI) catalysts prepared using conventional impregnation method and modified impregnation method. In modified impregnation method, oxoperoxo route was used to generate molybdenum(VI) peroxo complexes while polyoxo route was used as a conventional impregnation method using ammonium heptamolybdate,  $(\text{NH}_4)_6(\text{Mo}_7\text{O}_{24}) \cdot 4\text{H}_2\text{O}$  as a molybdenum precursor. They reported that impregnating molybdenum species using polyoxo route resulted in homogeneous molybdenum species distribution with the formation of  $\text{MoO}_3$  crystals of nanorods. However some zones were not covered. This drawback was overcome by using oxoperoxo route. Catalysts prepared using oxoperoxo route was active in the oxidation of (*R*)-(+)-limonene and only a small amount of molybdenum leached out. They had concluded that the interaction between  $\text{MoO}_3$  and  $\text{SiO}_2$  are weaker in the catalysts prepared using conventional impregnation method.

Zhao et al. (2009) tested the influence of tungsten content on the activity and selectivity of a series of tungsten-silica catalysts in the metathesis reaction between ethene and 2-butene to propene under conditions similar to industrial production. In industries, the reaction takes place at temperature  $> 553 \text{ K}$  and 30-35 bar. They had showed that tetrahedral active sites are more active in the metathesis reaction compared to octahedral tungsten species. The presence of  $\text{WO}_3$  crystals weakens the silica-tungsten interaction and did not participate in the reaction. The authors mentioned about catalysts deactivation. However, they did not provide further information.

#### 1.4.2 Direct hydrothermal method

Direct hydrothermal method is performed by adding metal ions directly into the mixture of support precursor before gellation takes place in the presence of heat (Lang et al., 2002). In the hydrothermal treatment, grain size, particle morphology, crystallinity, and surface chemistry can be controlled via processing variables such as sol composition, pH, reaction temperature and pressure, aging time, the nature of solvent and additive (Li et al., 2009).

Wang et al. (2003) prepared Cr-MCM-41 using direct hydrothermal method and tested the catalytic properties of the catalysts in the dehydrogenation of  $C_3H_6$  with  $CO_2$ . The catalysts showed 92-95 % of selectivity towards  $C_3H_6$ . They have speculated that the presence of aggregated  $Cr^{3+}$  species was responsible in catalyzing the reaction. The authors failed to provide any information on the reusability of the catalysts.

Miao et al. (2009) hydrothermally synthesized molybdenum silica meso-cellular foam (Mo-MCF) for the epoxidation of propylene by cumene hydroperoxide. The introduction of molybdenum did not destroy the meso structure of the support. Different types of molybdenum species such as isolated molybdenum species, polymolybdate species and crystalline  $MoO_3$  were detected on the catalysts. The group has identified that only isolated molybdenum species and polymolybdate species are responsible in catalyzing the reaction. However, no information were given on the reusability and leaching by the authors.

W-MCM-48 catalysts for the oxidation of cyclopentene to glutaraldehyde were synthesized by Yang et al. (2005) using hydrothermal method. Characterization of the catalyst indicates that tungsten has been uniformly incorporated inside the framework of MCM-48 support. They had also reported that

WO<sub>3</sub> crystals were embedded separately on the support and serve as active sites to catalyze the reaction. Even though tungsten species did not leached out from the support, longer reaction time and 50% hydrogen peroxide were required to achieve highest conversion and selectivity.

### **1.4.3 Sol-gel method**

Greater degree of control on the final properties of a catalyst can be tailor-made for a particular application by sol-gel method. This is due to the ability of metal precursor to be mixed homogeneously with the molecular precursor of the support under this preparation method (Lambert et al., 2001). Metal oxide with high purity can be formed because the polymerizing gel can trap metal ion components spatially, permitting precipitation from solution in which the entire metal ions occupy near-neighbour position in the gel matrix. Further processing and calcination decomposes the resultant amorphous mixture of metal oxide, hydroxides and metal salts leading to the formation M-O-M bond formation (Ying, 2001).

Oxidation of cyclohexane is an important process for the production of cyclohexanol and cyclohexanone. These two compounds are important intermediates in the manufacture of nylon-6 and nylon-66. Adam et al. (2009) and Sakthivel and Selvam (2002) prepared chromium-based catalysts using sol-gel and hydrothermal methods respectively. Both groups applied their catalysts in the oxidation of cyclohexane. Even though both preparation methods produced catalysts with good catalytic activity and selectivity, catalysts prepared by Adam et al. (2009) required less time to give maximum cyclohexane conversion compared to the catalysts prepared by Shaktivel and Selvam (2002).

Dai et al. (2001) prepared Mo-SBA-1 catalyst at 273 K using conventional impregnation method. They observed that the support's 3D channel network or cage-type pore structure with open window was partially destroyed upon the introduction of molybdenum. However, the pore structures were preserved when the same catalyst was prepared via sol-gel method by Wongkasemjit et al. (2009) at room temperature. Both catalysts have remarkable catalytic properties in oxidation reactions. However, no information on the leaching and reusability of the catalysts was given by both authors.

Somma and Strukul (2004) had successfully prepared a series of mesoporous tungsten oxide-silica mixed oxides catalysts using sol-gel technique under basic conditions. They reported that the catalysts were active in the oxidation of alcohol and resistant towards leaching due to the absence of  $\text{WO}_3$  crystal. Even though the catalysts were considered as an ultimate heterogeneous catalyst, tetramethoxysilane (TMOS) that was used as silica precursor was expensive and harmful.

## **1.5 Benzaldehyde**

Benzaldehyde is the simplest representative of aromatic aldehydes. Benzaldehyde is known to occur naturally as a glycoside called amygdalin. It was first isolated in 1803. In the 1830's, German chemists, Justus Von Leibig and Friedrich Wöhler investigated benzaldehyde in their studies leading towards the formation of structural theory of organic chemistry. The structure of amygdalin is given in Fig. 1.2.

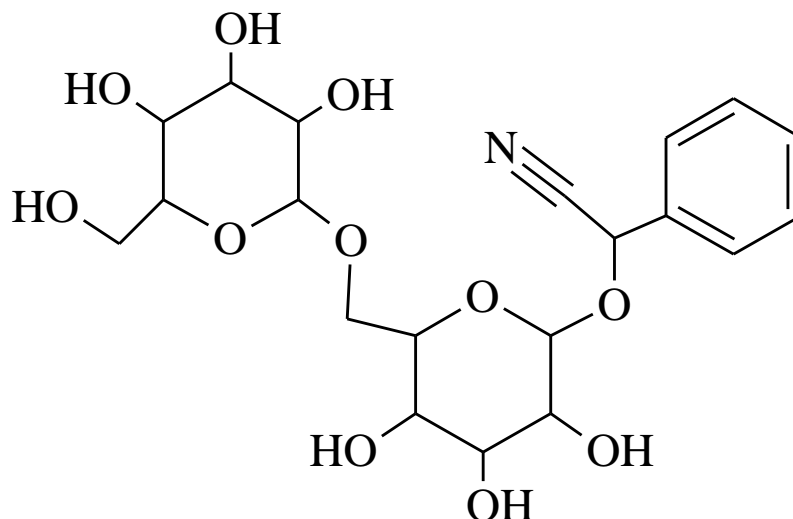


Fig. 1.2: The structure of amygdalin.

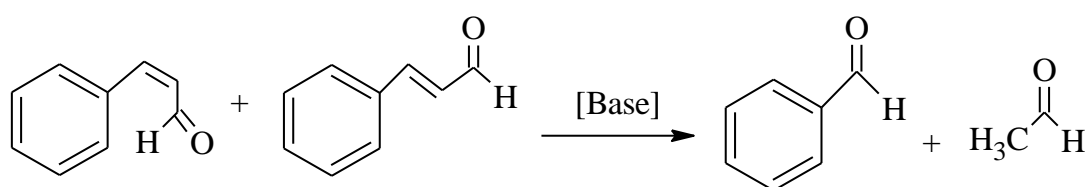
Benzaldehyde can be obtained from natural products or can be synthesized chemically. Benzaldehyde is a very useful starting material in the production of resin additives, dyes, flavours, and as an intermediate in pharmaceutical industries and in organic synthesis (Liu et al., 2010).

### 1.5.1 Benzaldehyde from natural sources

Prune, peach and apricot kernel have been known to contain significant amount of amygdalin for over a century. Reaction between amygdalin with water and enzymes yields benzaldehyde, hydrocyanic acid and glucose. However, benzaldehyde obtained from this process is not safe to be consumed due to the hydrocyanic acid contamination. It is known that uptake of hydrocyanic acid by human can be lethal (Scott & Scott, 1922).

In 1986, Wiener and Pitted had patented a synthesis route to prepare benzaldehyde from cinnamaldehyde. This process is done by refluxing *cis* or *trans*-cinnamaldehyde in aqueous/alcoholic solution for 5 to 80 h at 313 to 453 K using

base as a catalyst. Base catalysts that were used were sodium bicarbonate, potassium bicarbonate, sodium carbonate, potassium carbonate, lithium bicarbonate, lithium carbonate, magnesium hydroxide and calcium hydroxide. The pressure used was between 0.2 to 10 atm. The reaction scheme is shown in Scheme 1.1.



Scheme 1.1: Benzaldehyde preparation route from cinnamaldehyde.

## 1.5.2 Chemically-synthesized benzaldehyde

Synthetic benzaldehyde can be produced from the chlorination of toluene and oxidation of toluene. Some other processes that are known to produce benzaldehyde are partial oxidation of benzyl alcohol, reduction of benzoyl chloride and the reaction of carbon monoxide with benzene. However these processes are no longer practical to be applied in industries due to their low yield and by-products formation (Satrio & Doraiswamy, 2001).

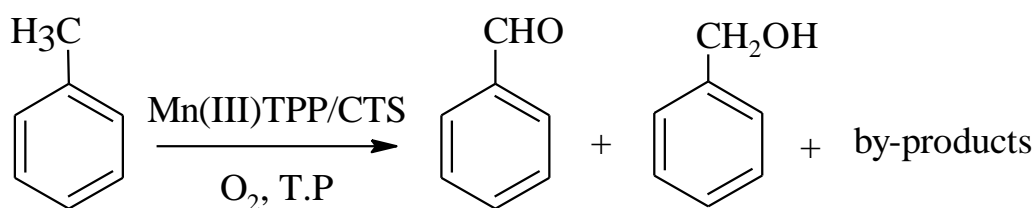
### 1.5.2.1 Chlorination of toluene

Since 1863, benzaldehyde was synthesized from the chlorination of the methyl group toluene. Benzal chloride that was derived from this chlorination process was later hydrolyzed to produce benzaldehyde (Pina et al., 2008). Benzaldehyde formed from this route does not meet the requirement for food and drug grade specification due to the contamination of chlorine. Dangerous waste such as hydrochloric acid generated from this process makes it least favorable from the environmental view point (Yongfei et al., 2007).

### 1.5.2.2 Catalytic oxidation of toluene

Catalytic oxidation of toluene in vapor or liquid phase is a famous method to obtain benzaldehyde synthetically. Most of the studies involved in catalytic oxidation of toluene are aided by transition metal containing catalysts.

Huang et al. (2008) had investigated the aerobic oxidation of toluene using manganese tetraphenylporphyrin supported on chitosan (Mn(III) TPP/CTS) as catalyst. Information on the physical properties of the catalysts was not given in details by the authors. The oxidation process was carried out in nitrogen charged autoclave and the pressure was maintained at 0.6 MPa at 468 K. The reaction pressure was also maintained by feeding air into the system at the flow rate of  $0.020 \text{ m}^3 \text{ h}^{-1}$ . No solvent or reductant was added into the reaction mixture. Benzaldehyde was obtained as the major product while benzoic acid and benzyl benzoate were the by-products. The conversion of toluene was 5.9 %. The authors did not state the exact selectivity of benzaldehyde. The selectivity was given by the authors in the form of aldehyde and alcohol mixture which was 96 %. The aerobic oxidation of toluene catalyzed by the catalysts is given in Scheme 1.2.

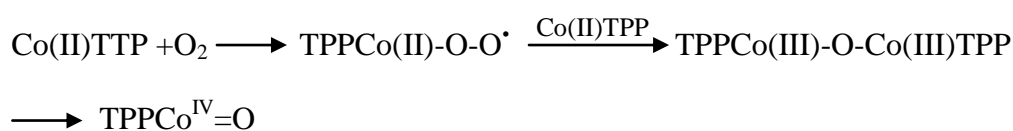


Scheme 1.2: Aerobic oxidation of toluene catalyzed by Mn(III)TPP/CTS catalyst.

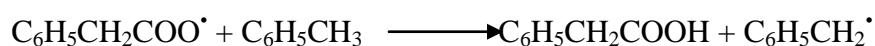
Guo et al. (2005) had prepared cobalt tetraphenylporphyrin Co(II)TTP and tested the capability of the catalyst to oxidize toluene under the general industrial conditions. Under the optimum conditions of 433 K, 0.8 MPa, and  $0.04 \text{ m}^3 \text{ h}^{-1}$

airflow, 8.9 % of toluene was converted with 33 % selectivity towards benzaldehyde. The conversion rate and selectivity rate were lower when the same reaction was carried out using cobalt acetate,  $\text{Co}(\text{OAc})_2$ . The amount of catalyst used was  $3.2 \times 10^{-5}$  M and the mole turnover number of the catalysts was about 25 000. The catalyst properties were not discussed in this paper. The authors proposed that the reaction was catalyzed by free radical-chain mechanism. The free radical mechanisms involved in the catalytic reaction as proposed by the authors is as follows:

Initiating:



Propagating:



Terminating:



Xue et al. (2007) had studied the relation between surface acidity and redox properties of V-Ag-Ni-O catalyst for the selective oxidation of toluene. From the study, they had identified that silver was capable of decreasing the surface acidity thus enhancing the redox properties of vanadium active sites. The addition of nickel further enhanced the catalytic activity. Oxidation of toluene carried out in a fixed-

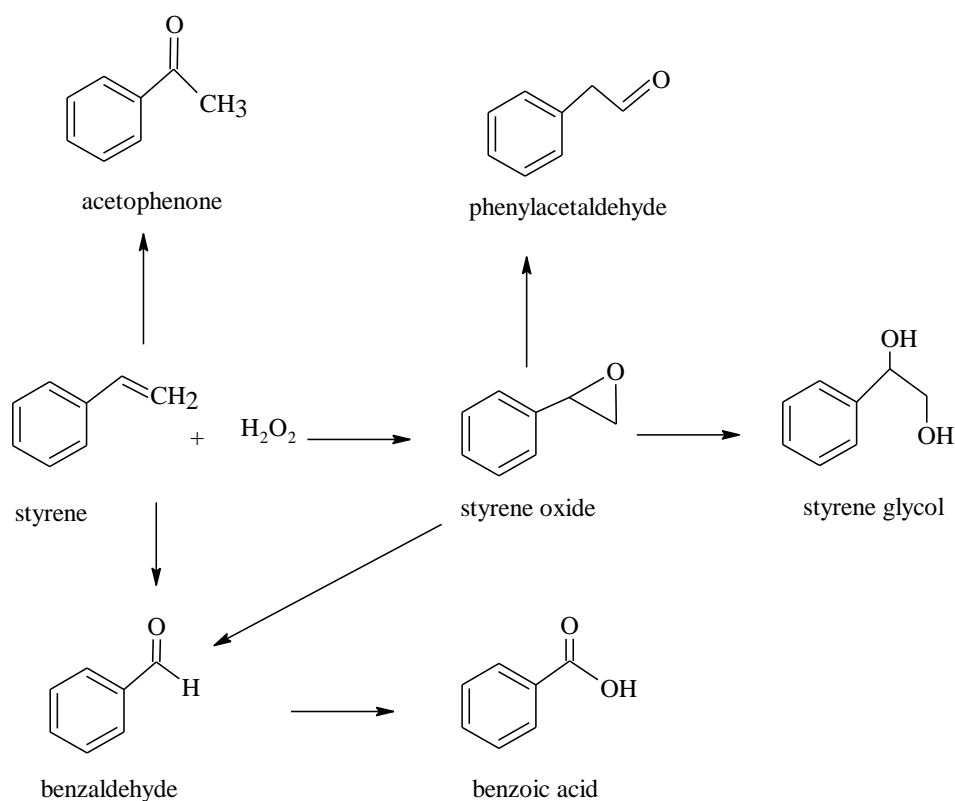
bed micro reactor converted 8 % of toluene to benzaldehyde at 613 K. The selectivity of benzaldehyde was 95 %.

Ge et al. (2007) had prepared a series of  $V_2O_5$  supported on  $ZrO_2$  complex oxides via sol-gel method for the catalytic oxidation of toluene. The main objective of their study was to identify the effect of surface acidity and redox properties of the catalysts on the oxidation process. Complex with low  $V_2O_5$  showed high surface acidity thus leading to lower selectivity towards benzaldehyde. The quality of the complex in catalyzing oxidation of toluene was improved in the presence of V-O-Zr bond. These bonds are capable of reducing the surface acidity and enhancing its redox properties. As a result, the catalysts were selective towards benzaldehyde. However, the authors did not provide any information on the surface acidity of the catalysts after catalytic activity. Analysis of surface acidity after catalytic activity is crucial in order to determine the stability of the catalysts. The authors also failed to provide information on leaching and reuseability.

### **1.5.2.3 Oxidation of styrene**

The oxidation of the side chain in styrene is of great interest in both academic and industry due to the formation of its oxide, ketone and aldehyde. Most researchers have concentrated on the production of styrene oxide compared to benzaldehyde. Often, benzaldehyde is regarded as an unwanted by-product. Only a few researchers had dedicated their research in manipulating styrene to produce benzaldehyde. The liquid phase oxidation of styrene can offer more environmentally friendly alternative route to produce benzaldehyde without the use of high pressure and temperature. Scheme 1.3 indicates the products of oxidation of styrene using

hydrogen peroxide as oxidant widely reported in literature. The formation of these products is discussed in Section 4.3.10.3.



Scheme 1.3: Products obtained from the oxidation of styrene using hydrogen peroxide.

Currently, the oxidation of an alkene into aldehyde and ketone is done in three ways: (1) by osmium tetroxide and ruthenium tetroxide in stoichiometric amount to cleave the C=C bond (2) by ozonolysis of the alkene to ozonides and subsequent conversion to aldehydes and ketones in reductive work up conditions, and (3) by using green oxidant (Nie et al., 2007). The use of osmium tetroxide involves the formation of highly toxic by-products while the multi-step ozonolysis are not cost effective. The most environmentally friendly and cost effective oxidant is molecular oxygen and hydrogen peroxide.

Molecular oxygen is very much desired by the industries because of its availability and low cost. However, molecular oxygen cannot be directly used because of the occurrence of auto-oxidation radical pathways making it less active. Organic reducing agents or sacrificial reductants such as alcohol or aldehyde need to be added to activate molecular oxygen (Tang et al., 2005). These reductants however cannot be recovered and are known to be co-oxidized to the corresponding organic acids that can contaminate products and create separation problems (Liu et al., 2004).

Hydrogen peroxide is another green oxidant that can be applied in the oxidation of styrene as a substitute for molecular oxygen. Compared to molecular oxygen, hydrogen peroxide has more active oxygen. It is easy to handle, safe and the only by-product that will be formed is water. Similar to molecular oxygen, hydrogen peroxide requires activation to increase its oxidation capability. The activation of hydrogen peroxide can be done by applying transition metal containing catalysts under various conditions.

Liu et al. (2009) had studied the nature of 3D worm-like holes mesoporous structure, Cr-MSU-1, and tested the catalytic activity of the catalysts in the oxidation of styrene. The reaction was carried out in a three-neck glass flask equipped with a magnetic stirrer and a reflux condenser. Even though the conversion of styrene was only 16.7 % in acetonitrile, the selectivity towards benzaldehyde was the highest at 83.1 %. They had also identified that  $\text{Cr}^{5+}$  and  $\text{Cr}^{6+}$  species in tetrahedral coordination are mainly responsible in catalyzing the reaction. By-products formed together with benzaldehyde are phenylacetaldehyde, benzoic acid, styrene oxide and styrene glycol. Even though the catalyst prepared was heterogeneous, the choice of silica precursor, TEOS, was expensive making the catalyst less desirable to be mass

produced. They had also added in NaF as a source of fluoride which has been classed as toxic by inhalation and digestion.

A series of Fe-MCM-41 were prepared by Zhang et al. (2003) using direct hydrothermal method and template ion exchange method. The reaction was carried out in batch type reactor at 343 K. The ratio of styrene/hydrogen peroxide used was 1:1 in dimethylformamide as solvent. Under these conditions, 3.5 to 13.8 % of styrene was converted in 2 h. The catalysts were selective towards styrene oxide instead of benzaldehyde. Selectivity towards benzaldehyde was 37.3-45.9 %. They showed that Fe-incorporated inside the MCM-41 framework was responsible in converting styrene to products while decomposition of hydrogen peroxide was facilitated by the iron oxide clusters formed. Data for leaching and the reusability of the catalysts were not reported in this paper.

The sol-gel method was used to prepare Fe and Ti-SBA-1 by Tanglumert et al. (2009). The catalysts were used to catalyze 10 mmol of styrene using 10 mmol of hydrogen peroxide in 10 mL of acetonitrile. It was found that 67 % of styrene was converted when 4% iron containing Fe-SBA-1 was used as catalyst. The selectivity towards benzaldehyde was 74 %. In addition, 69 % of styrene was converted when 2 % Ti-SBA-1 was used as catalyst which gave selectivity towards benzaldehyde of 50 %. They had concluded that the tetrahedrally coordinated and atomically isolated iron sites and  $\text{Ti}^{4+}$  incorporated inside the framework were responsible in catalyzing the reaction. The authors did not provide any discussion on the stability of the catalysts in terms of leaching and reuseability.

Oxovanadium(IV), dioxomolybdenum(VI) and copper(II) have been immobilized on polymer support using very tedious multi steps synthesis and tested in the oxidation of styrene. Oxovanadium(IV) immobilized on polymer showed the

highest styrene conversion, 81 % with 62.6 % of benzaldehyde selectivity. However, only 68.0 % of styrene was converted with 66.0% selectivity towards benzaldehyde when dioxomolybdenum(VI) was used. The lowest conversion, 57.0 %, was achieved when copper(II) immobilized on polymer was used as the catalyst. The selectivity towards benzaldehyde was 63.7 %.

The authors had presented three possible reaction paths for the oxidation of styrene promoted by the catalysts. Even though benzaldehyde was reported as the major product, the authors did not indicate how benzaldehyde was formed in their reaction mechanisms.

In all cases, the  $V^{IV}$ - complexes were oxidized to  $V(V)O_2$ -complex which then reacted with hydrogen peroxide. The  $V(V)O_2$ -complexes were reduced to  $V(IV)$ -complex by the styrene when hydrogen peroxide was consumed. For molybdenum and copper metal active centers, the cores can be substituted by  $Cu(II)$  (or  $Mo(VI)O$  and  $Mo(VI)O_2$ ), and the initial and final oxidation steps ( $V(IV) \rightarrow V(V)$ ) do not exist.

In the first alternative, the authors had proposed the formation of vanadium-peroxy-styrene intermediate upon the attack of the styrene to the transient vanadyl diradical species ( $O=V(IV)-O-O\bullet$ ). The breakage of bond between oxygen atom led to the formation of styrene oxide. The reaction path is shown in Scheme 1.4.